

## Steam injection into water-saturated porous rock

J. BRUINING<sup>1</sup>, D. MARCHESIN<sup>2</sup> and C.J. VAN DUIJN<sup>3</sup>

<sup>1</sup>Dietz Laboratory, Centre of Technical Geoscience, Mijnbouwstraat 120  
2628 RX Delft, The Netherlands

E-mail: J.Bruining@mp.tudelft.nl

<sup>2</sup>Instituto Nacional de Matemática Pura e Aplicada, Estrada Dona Castorina 110  
22460-320 Rio de Janeiro, RJ, Brazil

E-mail: marchesi@impa.br

<sup>3</sup>Technische Universiteit Eindhoven, Den Dolech 2  
5600 MB Eindhoven, The Netherlands

E-mail: c.j.v.duijn@tue.nl

---

**Abstract.** We formulate conservation laws governing steam injection in a linear porous medium containing water. Heat losses to the outside are neglected.

We find a complete and systematic description of all solutions of the Riemann problem for the injection of a mixture of steam and water into a water-saturated porous medium. For ambient pressure, there are three kinds of solutions, depending on injection and reservoir conditions. We show that the solution is unique for each initial data.

**Mathematical subject classification:** 76S05, 35L60, 35L67.

**Key words:** porous medium, steamflood, travelling waves, multiphase flow.

---

### Introduction

Steam injection is an effective technique to restore groundwater aquifers contaminated with non-aqueous phase liquids (NAPL's) such as hydrocarbon fuels and halogenated hydrocarbons [15]. It is also one of the most effective methods to

---

#558/02. Received: 28/XII/02. Accepted: 18/VIII/03.

This work was supported in part by: CNPq under Grant 301532/2003-6, FINEP under CT-PETRO Grant 21.01.0248.00; NWO under Fellowship Grant R 75-389, The Netherlands; IMA (Univ. of Minnesota), and therefore by NSF, Dietz Laboratory (TU Delft, The Netherlands), IMPA (Brazil).

recover oil from medium to heavy oil reservoirs [13]. The main feature of steam injection is the steam condensation front (*SCF*), which marks the boundary between the upstream zone at boiling temperature and the downstream liquid zone below the boiling temperature. Depending on the situation there may exist an isothermal steam-water shock at the boiling temperature (*HISW*) instead of the *SCF*. The main result of this work is a complete and systematic classification of the structure of all possible cases of Riemann solutions. As a first step we have ignored the presence of NAPL's in our model. The model has also applications outside the use of steam for oil recovery or pollutant product recovery, for example in chemical engineering.

There is an extensive literature on models of steam drive. Their main focus is the internal structure of the steam condensation front and they are reviewed in [4], [5].

In this article we limit ourselves to the simple case of steam displacing water. Our aim is to investigate a unique well posed solution of the Riemann problem for all possible values of the model parameters, providing mathematical validation of our model. This is the first step towards solving the full problem of groundwater NAPL removal.

In Section 1, the physical model is presented. It is described mathematically by balance equations of mass and thermal energy, which are rewritten into a form suitable for analysis.

Section 2 presents the basic waves arising in the model; the main concern is to identify their speeds, so as to be able to find the order in which they may appear in a linear steam injection experiment. In Section 3, we see that for certain values of initial and boundary data, some of these speeds coincide, giving rise to bifurcation and structural change in the Riemann solution. All solutions of the Riemann problem are in Section 4. Section 5 verifies that the *SCF* satisfies Lax's shock inequalities, but not strictly. Section 6 summarizes our results and conclusions.

Appendix A describes notation and values for the physical quantities appearing in the model.

## 1 Physical and mathematical model

### 1.1 Physical model

We consider linear steam displacement in a homogeneous reservoir of constant permeability and porosity. The reservoir is initially saturated with water. The pressure gradients  $\partial p_w / \partial x$ ,  $\partial p_g / \partial x$  driving the fluids are small with respect to the prevailing system pressure  $p$  divided by the length of the reservoir. In particular, within the short steam condensation zone pressure variations are negligible. Hence we disregard the effect of pressure variation on the density of the fluids and on their thermodynamic properties. The reservoir is horizontal, so gravitational effects vanish.

A steam-water mixture is injected at constant rate  $u^{inj}$  and constant steam/water injection ratio. Transverse heat losses are disregarded. We neglect capillary forces after steam breakthrough at the production end of the reservoir to avoid problems with the capillary end effect, which is outside the present scope of our interest.

The effects of temperature on the fluid properties, *e.g.* water viscosity  $\mu_w$ , steam viscosity  $\mu_g$ , water density  $\rho_w$  and steam density  $\rho_g$  are taken into account. Darcy's Law determines the fluid motion. The temperature dependence of heat capacities and of the evaporation heat are also taken into account. Capillary pressure as well as an effective longitudinal heat *conduction* term are included.

We have chosen to describe condensation in terms of a steam mass condensation rate equation. The mass condensation rate  $q$  is always positive when the temperature drops below the boiling temperature  $T^b$  as long as not all steam has condensed, that is  $S_w < 1$ .

The stated conditions can be considered representative of steam injection in the subsurface for remediation of contaminated sites. As steam is injected the reservoir is heated. Depending on the proportions of steam and water in the injected mixture, we can distinguish three regimes, which differ in the structure of Riemann solutions. When pure steam is injected, there will be a decrease of the steam saturation in the hot zone away from the injection point, described as a rarefaction wave, and then a *SCF* to the cold water, described as a shock with a concentrated source term. This is called situation *I*. As the water injection

rate is increased further a zone in which the steam saturation is constant will develop preceding the rarefaction wave until the steam saturation in the hot zone is constant. After this constant state there is a *SCF* and a cold water region. This will be called situation *II*. Finally when the water–steam injection ratio is increased further, the steam bank will not be fast enough to reach the cooling front separating the hot and cold water zones; thus there is no *SCF*. This and higher ratios originate in situation *III*. In all regimes, there is a hot zone and a cool zone, whose boundary moves with constant speed, as shown in Fig. 1.

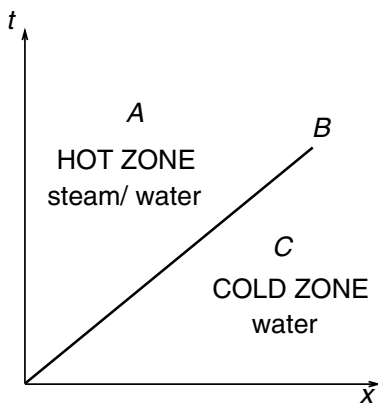


Figure 1 – B: Condensation front or cooling front.

Each of the enthalpies per unit volume  $H_w(T)$ ,  $H_r(T)$ ,  $H_g(T)$  ( $[J/m^3]$ ) is defined with respect to the enthalpy at the initial reservoir temperature  $T^0$  at the standard state. This means that they are all zero at the initial temperature  $T^0$ . The enthalpy of steam is subdivided in a sensible part  $H_g^s(T)$  and a latent part  $H_g^l(T^0)$ , *i.e.*  $H_g(T) = H_g^s(T) + H_g^l(T^0)$ . The sensible heat  $H_g^s(T^0)$  is zero at the initial reservoir temperature. The evaporation heat or the latent heat per unit mass at the initial reservoir temperature  $T^0$  is denoted by

$$\Lambda^0 = \Lambda(T^0) = H_g^l(T^0)/\rho_g(T^0). \quad (1)$$

In general  $\Lambda(T)$  is the evaporation heat per unit mass at temperature  $T$ . The enthalpies as a function of temperature are summarized in Appendix A for convenience.

We assume Darcy’s law for two-phase flow, water and steam respectively, without gravity terms:

$$u_w = -\frac{kk_{rw}}{\mu_w} \frac{\partial p_w}{\partial x}, \quad u_g = -\frac{kk_{rg}}{\mu_g} \frac{\partial p_g}{\partial x}. \tag{2}$$

The liquid water viscosity and the steam viscosity are temperature-dependent functions (see Appendix A).

As discussed in [4], the water mass source term is taken as

$$q = \begin{cases} q_b(T - T^b)(S_w - 1) & \text{for } T \leq T^b, \quad 0 \leq S_w \leq 1; \\ 0 & \text{otherwise.} \end{cases} \tag{3}$$

This term is motivated by the idea that the condensation rate is determined by a ‘‘driving force’’ which is proportional to its departure from equilibrium  $S_w = 1$  and  $T = T^b$  ( see also reference [11]). The value of  $q_b$  is considered very large.

### 1.2 The model equations

The mass balance equation of liquid water and steam read as follows:

$$\frac{\partial(\varphi\rho_w S_w)}{\partial t} + \frac{\partial(\rho_w u_w)}{\partial x} = q, \tag{4}$$

$$\frac{\partial(\varphi\rho_g S_g)}{\partial t} + \frac{\partial(\rho_g u_g)}{\partial x} = -q. \tag{5}$$

The rock porosity  $\varphi$  is assumed to be constant. We include longitudinal heat conduction, but neglect heat losses to the surrounding rock, in the energy balance equation given below. By our assumption of almost constant pressure we ignore adiabatic compression and decompression effects. Thus the energy balance is (See reference [2], Table 10.4-1):

$$\frac{\partial}{\partial t}(H_r + \varphi S_w H_w + \varphi S_g H_g) + \frac{\partial}{\partial x}(u_w H_w + u_g H_g) = \frac{\partial}{\partial x} \left( \kappa \frac{\partial T}{\partial x} \right). \tag{6}$$

Here  $\kappa$  is the composite conductivity of the rock–fluid system [1]:

$$\kappa = \kappa_r + \varphi(S_w \kappa_w + S_g \kappa_g). \tag{7}$$

Equations (4), (5), and (6) are the basic governing equations for the flow.

Equations (4) and (5) are combined with the heat balance equation (6), where we also use separation in sensible and latent quantities, to obtain:

$$\begin{aligned} \frac{\partial}{\partial t} (H_r + \varphi S_w H_w + \varphi S_g H_g^s) + \frac{\partial}{\partial x} (u_w H_w + u_g H_g^s) - \frac{\partial}{\partial x} \left( \kappa \frac{\partial T}{\partial x} \right) \\ = -\frac{\partial}{\partial t} (\varphi S_g H_g^l) - \frac{\partial}{\partial x} (u_g H_g^l) = -\frac{\partial}{\partial t} (\varphi S_g \rho_g \Lambda^0) - \frac{\partial}{\partial x} (u_g \rho_g \Lambda^0) \\ = -\Lambda^0 \left( \frac{\partial}{\partial t} (\varphi S_g \rho_g) + \frac{\partial}{\partial x} (u_g \rho_g) \right). \end{aligned}$$

Using Eq. (5), this yields

$$\begin{aligned} \frac{\partial}{\partial t} (H_r + \varphi S_w H_w + \varphi S_g H_g^s) + \frac{\partial}{\partial x} (u_w H_w + u_g H_g^s) \\ = q \Lambda^0 + \frac{\partial}{\partial x} \left( \kappa \frac{\partial T}{\partial x} \right). \end{aligned} \quad (8)$$

Let us define the fractional flow functions for water and steam:

$$f_w = \frac{k_{rw}/\mu_w}{k_{rw}/\mu_w + k_{rg}/\mu_g}, \quad f_g = \frac{k_{rg}/\mu_g}{k_{rw}/\mu_w + k_{rg}/\mu_g}. \quad (9)$$

The capillary pressure

$$P_c = P_c(S_w) = p_g - p_w \quad (10)$$

which is given by Equation (83), is a strictly monotone decreasing function; it appears in the definition of the capillary diffusion coefficient  $\Omega$ :

$$\Omega = -f_w \frac{k k_{rg}}{\mu_g} \frac{dP_c}{dS_w} \geq 0. \quad (11)$$

We notice that  $\Omega$  vanishes precisely at water saturations  $S_w = S_{wc}$  and  $S_w = 1$ .

Using Darcy's law (2) (in the absence of gravitational effects) and the definition of  $P_c$  given in Eq. 10, one can easily show from Eqs. (2) and (11) that:

$$u_w = u f_w - \Omega \frac{\partial S_w}{\partial x}, \quad u_g = u f_g - \Omega \frac{\partial S_g}{\partial x}, \quad (12)$$

where

$$u = u_w + u_g \quad (13)$$

is the *total* or *Darcy velocity* and  $\Omega$  acts as a saturation-dependent capillary diffusion coefficient.

Substituting (12) into Equations (4), (5) and (8) leads to

$$\varphi \frac{\partial (\rho_w S_w)}{\partial t} + \frac{\partial (\rho_w u f_w)}{\partial x} = q + \frac{\partial}{\partial x} \left( \rho_w \Omega \frac{\partial S_w}{\partial x} \right), \tag{14}$$

$$\varphi \frac{\partial (\rho_g S_g)}{\partial t} + \frac{\partial (\rho_g u f_g)}{\partial x} = -q + \frac{\partial}{\partial x} \left( \rho_g \Omega \frac{\partial S_g}{\partial x} \right), \tag{15}$$

$$\begin{aligned} \frac{\partial}{\partial t} (H_r + \varphi H_w S_w + \varphi H_g^s S_g) + \frac{\partial}{\partial x} \left( u (H_w f_w + H_g^s f_g) \right) \\ = q \Lambda^0 + \frac{\partial}{\partial x} \left( (H_w - H_g^s) \Omega \frac{\partial S_w}{\partial x} \right) + \frac{\partial}{\partial x} \left( \kappa \frac{\partial T}{\partial x} \right). \end{aligned} \tag{16}$$

The governing system of equations is (14)–(16).

As to initial conditions, we assume that the reservoir is filled with water at saturation  $S_w(x, t = 0) = S_w^0 = 1$  with constant temperature  $T(x, t = 0) = T^0$ . As to boundary conditions, the total injection rate  $u^{inj}$  is specified and constant (see Appendix A). The constant steam-water injection ratio is specified in terms of the water saturation  $S_w^{inj}$  at the injection side.

**Lemma 1.** *In a region where the temperature is constant (and noncritical),  $q = 0$ .*

**Proof.** If the temperature is constant, the enthalpies are constant, so Eq. (8) becomes

$$\varphi H_w \frac{\partial S_w}{\partial t} + \varphi H_g^s \frac{\partial S_g}{\partial t} + H_w \frac{\partial u_w}{\partial x} + H_g^s \frac{\partial u_g}{\partial x} = q \Lambda^0. \tag{17}$$

We regroup Eq. (17) and use the mass balance equations (4) and (5). Since the temperature is constant the densities are constant too, so Eq. (17) becomes

$$\begin{aligned} H_w \left( \varphi \frac{\partial S_w}{\partial t} + \frac{\partial u_w}{\partial x} \right) + H_g^s \left( \varphi \frac{\partial S_g}{\partial t} + \frac{\partial u_g}{\partial x} \right) = q \Lambda^0, \\ \frac{H_w}{\rho_w} q - \frac{H_g^s}{\rho_g} q = q \Lambda^0, \quad \left( \frac{H_w}{\rho_w} - \frac{H_g^s}{\rho_g} - \Lambda^0 \right) q = 0. \end{aligned} \tag{18}$$

The term in parenthesis in Eq. (18) is minus the enthalpy per unit mass required to convert water into steam and is therefore non-zero. Consequently we must have that  $q = 0$ . Summarizing, we can say that if the temperature is constant in space and time then there is no source term.  $\square$

**Remark 1.** It is easy to see that the source term  $q$  vanishes in regions where either (i) the temperature is constant, (ii) the gas saturation is zero, (iii) the water saturation is zero.

## 2 The hyperbolic framework

By ignoring capillary pressure and heat conduction diffusive effects, we are in the framework of first order hyperbolic conservation laws; this framework is useful to study the basic waves of the model. Throughout this section we assume that all fluids are in thermodynamic equilibrium. Equations (14) and (15), the mass balance equation of liquid water and steam combined with Darcy's law read as follows:

$$\frac{\partial(\varphi\rho_w S_w)}{\partial t} + \frac{\partial(\rho_w u f_w)}{\partial x} = q, \quad (19)$$

$$\frac{\partial(\varphi\rho_g S_g)}{\partial t} + \frac{\partial(\rho_g u f_g)}{\partial x} = -q. \quad (20)$$

When we add these equations, we obtain the total water conservation:

$$\varphi \frac{\partial}{\partial t} (\rho_w S_w + \rho_g S_g) + \frac{\partial}{\partial x} \left( u(\rho_w f_w + \rho_g f_g) \right) = 0. \quad (21)$$

Eq. (16) becomes

$$\frac{\partial}{\partial t} (H_r + \varphi H_w S_w + \varphi H_g^s S_g) + \frac{\partial}{\partial x} \left( u(H_w f_w + H_g^s f_g) \right) = q \Lambda^0, \quad (22)$$

or equivalently, as in Eq. (6)

$$\frac{\partial}{\partial t} (H_r + \varphi H_w S_w + \varphi H_g S_g) + \frac{\partial}{\partial x} \left( u(H_w f_w + H_g f_g) \right) = 0. \quad (23)$$

Eqs. (21) and (22) will be used for most of the analysis in this section.

**Remark 2.** Notice that all speeds defined by Equations (21) and (22) are proportional to  $u$ . Thus we can choose any speed to parameterize all the other ones.

Let us consider all regions where the mass transfer term vanishes. The mass transfer can vanish because of several reasons. Based on these reasons, we classify the regions in the following table. Because the mass source term vanishes (Eq. (3)), we have the following zones in the reservoir:

$S_w \backslash T$	$T = T^b$	$T < T^b$
$S_w < 1$	hot steam zone	XXXXXXXXXXXXXX
$S_w = 1$	hot water zone	cold water zone

Table 1 – Classification according to mass source term.

We call ‘‘hot steam-water region’’, or ‘‘hot region’’, the hot steam zone together with hot water zone, where  $T = T^b$ . We call ‘‘liquid water region’’ the hot water zone together with the cold water zone.

These regions overlap on the hot water zone.

**Remark 3.** There is no ‘‘cold steam zone’’ in Table 1 because at thermodynamical equilibrium steam cannot exist at a temperature lower than  $T^b$ .

As we will see, a configuration composed by sequential zones of hot steam, hot water and cold water is possible, counting away from the injection point. At the first interface  $S_w = 1$  is reached, while at the second one  $T = T^0$  is reached.

A configuration containing only the hot steam zone and the cold water zone is possible if we interpose the so called *SCF*, where both saturation and temperature change abruptly.

**Lemma 2.** *The source term in the hot region and in the liquid water region is zero. That the source term is zero in the hot region follows from Remark 1. That the source term is zero in the liquid region follows from the existence of a single phase and consequent absence of mass and energy transfer between phases.*

## 2.1 The hot region

This region starts with the hot steam zone, where steam is injected at boiling temperature  $T^b$ . We claim that the Darcy velocity  $u$  (given by Eq. (13)) in the hot region is independent of position. To prove this fact we use equations (19), (20). As the temperature is  $T^b$ , the source term (such as given in Eq. (3)) vanishes and the densities are constant. We can divide Eqs. (19), (20) by the densities and add the resulting equations and obtain our claim.

Since the Darcy velocity  $u$  is a constant in space in the hot region and since in this work we also take that  $u^{inj}$  is constant in time, the temperature  $T^b$  and the Darcy velocity  $u^b$  are constant in this region. Thus Eq. (22) is satisfied trivially, and both Eqs. (19) and (20) reduce to any of the two equivalent forms of the Buckley-Leverett problem for steam and water that follows:

$$\varphi \frac{\partial S_w}{\partial t} + u^b \frac{\partial f_w}{\partial x} = 0, \quad \varphi \frac{\partial S_g}{\partial t} + u^b \frac{\partial f_g}{\partial x} = 0. \quad (24)$$

This equation governs propagation in the hot steam zone, as long as steam and water are both present. The classical Oleřnik construction [10], or equivalently, the fractional flow theory [12] describe waves in this zone.

We will denote by  $v_s^b$  the speed of propagation of saturation waves in the hot steam zone. It is obtained from Eq. (24) as the characteristic speed:

$$v_s^b = v_s^b(S_w; u^b) = \frac{u^b}{\varphi} \frac{\partial f_w^b}{\partial S_w}(S_w), \quad (25)$$

where  $T = T^b$  and we use the nomenclature  $f_w^b(S_w) = f_w(S_w, T^b)$ .

A particular Buckley-Leverett shock for (24) turns out to play a relevant role, separating a mixture of steam and water from pure water, both at boiling temperature. We call it the *hot isothermal steam-water shock* or *HISW* shock between the (−) state  $(S_w^b, T^b, u^b)$  containing steam and the (+) state  $(1, T^b, u^b)$  containing water at boiling temperature. It has speed  $v_{g,w}^b$  given by

$$v_{g,w}^b = v_{g,w}^b(S_w^b; u^b) = \frac{u^b}{\varphi} \frac{f_g^b(S_g^b)}{S_g^b} = \frac{u^b}{\varphi} \frac{1 - f_w^b(S_w^b)}{1 - S_w^b}. \quad (26)$$

Notice that, because  $f_g(S_g = 0) = 0$  and  $(\partial f_g / \partial S_g)(S_g = 0) = 0$  from Eq. (9) and from the quadratic behavior of the steam relative permeabilities in the

saturation given in Eq. (82), with  $n_g = 2$  we obtain:

$$v_{g,w}^b(S_w = 1; u^b) = 0. \tag{27}$$

Similarly, for  $S_w^b \leq S_{wc}$  from Eqs. (82) and (9),

$$v_{g,w}^b = \frac{u^b}{\varphi(1 - S_w^b)} > 0. \tag{28}$$

**Remark 4.** It is easy to verify that  $v_s^b$  in Eq. (25) is monotonously increasing in  $S_w^b$  when  $S_w^b$  is less than  $S^{infl}$ , the inflection abscissa of  $f_w$ , and monotonously decreasing when  $S_w^b$  is larger than  $S^{infl}$ .

### 2.2 Liquid water region

We recall that the liquid water zone consists of the hot region, which is also part of the hot region examined in Section 2.1, and of the cold water zone.

In the liquid water zone there is no steam, so there is no mass transfer between steam and water. So  $q = 0$ . Also, in the liquid region  $S_w = 1$ , so Eqs. (21) and (22) reduce to

$$\varphi \frac{\partial \rho_w}{\partial t} + \frac{\partial(u\rho_w)}{\partial x} = 0, \tag{29}$$

$$\frac{\partial}{\partial t}(H_r + \varphi H_w) + \frac{\partial(uH_w)}{\partial x} = 0. \tag{30}$$

#### 2.2.1 Cooling contact discontinuity

We will assume that  $\rho_w$  and  $C_w^p$  are essentially constant in the pressure and temperature region of interest. A more complete discussion can be found in [5].

Let us consider a temperature discontinuity from  $T^b$  to  $T^0$ , with speed  $v_w^{b,0}$  in the liquid water between the hot left (or upstream) state ( $S_w = 1, T = T^b, u^b$ ) and the cold right (or downstream) state ( $S_w = 1, T = T^0, u^0$ ). For such a *cooling contact discontinuity*, from Eqs. (29) and (30) one can obtain the following Rankine-Hugoniot relation, where we denote by  $u^b$  and  $u^0$  the Darcy velocities at the discontinuity sides corresponding to  $T^b$  and  $T^0$ :

$$v_w^{b,0} = \frac{u^0 \rho_w^0 - u^b \rho_w^b}{\varphi(\rho_w^0 - \rho_w^b)} = \frac{u^0 H_w^0 - u^b H_w^b}{(H_r^0 + \varphi H_w^0) - (H_r^b + \varphi H_w^b)}, \tag{31}$$

where

$$H_w^b = H_w(T^b), \quad H_r^b = H_r(T^b), \quad \rho_w^b = \rho_w(T^b). \quad (32)$$

We recall that our convention is that enthalpies vanish at  $T^0$ ; then the Rankine-Hugoniot condition can be rewritten as

$$v_w^{b,0} = \frac{u^0 \rho_w^0 - u^b \rho_w^b}{\varphi(\rho_w^0 - \rho_w^b)} = u^b \frac{H_w^b}{H_r^b + \varphi H_w^b}. \quad (33)$$

From the second equality in Eq. (33), we obtain that

$$u^b = \frac{H_r^b + \varphi H_w^b}{H_r^b \rho_w^b / \rho_w^0 + \varphi H_w^b} u^0, \quad (34)$$

which expresses the conservation of water mass.

From the last term in Eq. (33) and from Eq. (34):

$$v_w^{b,0} = \frac{H_w^b}{H_r^b \rho_w^b / \rho_w^0 + \varphi H_w^b} u^0. \quad (35)$$

**Remark 5.** Notice that the dependence of  $\rho_w$  on temperature is often small. If  $\rho_w$  were independent of temperature (constant), then Eq. (34) would imply that  $u^b = u^0$ .

**Remark 6.** Since all speeds in this problem scale with  $u$ , and  $u^{inj}$  is constant in time,  $u^0$  and  $u^b$  are constant in time.

**Remark 7.** In the hot water zone, both  $S_w = 1$  and  $T = T^b$ , so  $q = 0$ . Since the temperature is constant, so is  $\rho_w$ , thus Eq. (29) says that  $u$  is a constant, which has already been called  $u^b$  in Section 2.1. Equation (30) says that the characteristic speed (of temperature waves) in the hot water zone is

$$v_w^b = \frac{C_w^p(T^b)}{C_r^p(T^b) + \varphi C_w^p(T^b)} u^b. \quad (36)$$

This is the propagation speed of small temperature perturbations near  $T = T^b$  in the hot water zone.

**Remark 8.** Under the assumptions that  $\rho_w$  and  $C_w^p$  are constant in pressure and temperature, the characteristic speeds (36) evaluated at  $T^b$ , and evaluated at  $T^0$  coincide with the discontinuity speed (31). In gas dynamics, discontinuities with this coincidence property are called contact discontinuities. Hence the name we gave to this wave.

### 2.3 Steam condensation front

This is a discontinuity joining a state  $(-)$  containing steam and water at temperature  $T^b$  to pure water at temperature  $T^0$ , a state  $(+)$ ; that is, it separates the hot steam zone from the cold water zone. It satisfies the following Rankine-Hugoniot conditions with speed  $v^{SCF}$  for Eqs. (21), (23) between states  $(S_w^b, T^b, u^b)$  and  $(S_w^0 = 1, T^0, u^0)$ . From the water balance (21) we obtain:

$$\begin{aligned}
 u^b (\rho_w f_w + f_g \rho_g)^- - \varphi v^{SCF} (\rho_w S_w + S_g \rho_g)^- \\
 = u^0 (\rho_w f_w + f_g \rho_g)^+ - \varphi v^{SCF} (\rho_w S_w + S_g \rho_g)^+
 \end{aligned}
 \tag{37}$$

and from the energy balance (23) we obtain:

$$\begin{aligned}
 u^b (H_w f_w + H_g f_g)^- - v^{SCF} (H_r + \varphi H_w S_w + \varphi H_g S_g)^- \\
 = u^0 (H_w f_w + H_g f_g)^+ - v^{SCF} (H_r + \varphi H_w S_g + \varphi H_g S_g)^+.
 \end{aligned}
 \tag{38}$$

As no steam exists on the right of the  $SCF$ , we can say that  $S_w^0 = f_w^0 = 1$  and  $S_g^0 = f_g^0 = 0$  and thus Eq. (37) becomes

$$u^b (\rho_w f_w + \rho_g f_g)^- - \varphi v^{SCF} (\rho_w S_w + \rho_g S_g)^- = \rho_w^0 (u^0 - \varphi v^{SCF}). \tag{39}$$

Under the same conditions we obtain for the heat balance equation (38):

$$\begin{aligned}
 u^b (H_w f_w + H_g f_g)^- - v^{SCF} (H_r + \varphi H_w S_w + \varphi H_g S_g)^- \\
 = u^0 H_w^0 - v^{SCF} (H_r^0 + \varphi H_w^0) = 0.
 \end{aligned}
 \tag{40}$$

The RHS term of Eq. (40) vanishes in the absence of steam because of our convention for enthalpies, as far as rock and water are concerned. For the  $SCF$

velocity it follows from Eqs. (39), (40) that

$$u^0 = u^b \left( \frac{\rho_g^b}{\rho_w^b} f_g^b + \frac{\rho_w^b}{\rho_w^b} f_w^b \right) - \varphi v^{SCF} \left( \frac{\rho_g^b}{\rho_w^0} S_g^b + \frac{\rho_w^b}{\rho_w^0} S_w^b - 1 \right), \tag{41}$$

$$v^{SCF} = u^b \frac{H_w^b f_w^b + H_g^B f_g^b}{H_r^b + \varphi H_w^b S_w^b + \varphi H_g^B S_g^b}, \tag{42}$$

where we used the nomenclature that follows from Eq. (1):

$$H_g^B \equiv H_g(T^b) = H_g^s(T^b) + H_g^l = H_g^b + \Lambda^0 \rho_g^0. \tag{43}$$

Because  $S_g^b = 1 - S_w^b$ ,  $f_g^b = 1 - f_w^b$  and  $f_w^b$  depends only on the water saturation in the constant temperature steam zone, we observe that  $u^0$  depends only on the water saturation and the Darcy velocity at the left of the *SCF* as well as on the velocity of the *SCF*.

From Eqs. (41) and (42), we can write  $u^0$  in terms of  $u^b$ :

$$\begin{aligned} \frac{u^0}{u^b} &= \left( \frac{\rho_w^b}{\rho_w^0} f_w^b + \frac{\rho_g^b}{\rho_w^0} f_g^b \right) \\ &- \varphi \left( \frac{\rho_w^b}{\rho_w^0} S_w^b + \frac{\rho_g^b}{\rho_w^0} S_g^b - 1 \right) \frac{H_w^b f_w^b + H_g^B f_g^b}{H_r^b + \varphi H_w^b S_w^b + \varphi H_g^B S_g^b}. \end{aligned} \tag{44}$$

Eqs. (42) and (44) represent the speeds  $v^{SCF}$  and  $u^0$  in terms of  $u^b$ . Eq. (44) easily allows to read  $u^b$  in terms of  $u^0$  (see Figure 2). We can use the expression of  $\left[ \frac{u^0}{u^b} \right]$  given by Eq. (44) in Eq. (42) to obtain  $v^{SCF}$  in terms of  $u^0$ :

$$v^{SCF} = u^0 \left[ \frac{u^0}{u^b} \right]^{-1} \frac{H_w^b f_w^b + H_g^B f_g^b}{H_r^b + \varphi H_w^b S_w^b + \varphi H_g^B S_g^b}. \tag{45}$$

Finally, we replace  $H_g^B$  in Eq. (45) by its definition given in Eq. (43).

**Remark 9.** In principle, (+) states with temperature  $T$  different from  $T^0$  could be considered, but because  $C_w^p$  was assumed to be constant such condensation discontinuities do not appear in the Riemann solution.

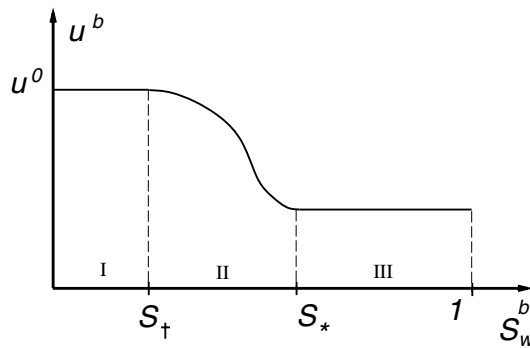


Figure 2 – Speed  $u^b$  versus  $S_w^b$  for fixed  $T^0, u^0$ , obtained from Eq. (44). The curve is almost horizontal at  $S_*$ ; if  $\rho_g$  and  $H_g^B$  could be neglected, and  $\rho_w$  were independent of temperature, tangency of the left and right curves at  $S_*$  would be exact (using Eq. (47)).

### 2.4 Cold water zone

In the cold water zone,  $S_w = 1$ , so  $q = 0$ . Since  $T = T^0$  is constant, so is  $\rho_w$ . Thus Eq. (29) says that  $u$  is a constant that has been called  $u^0$ . Equation (30) says that the characteristic speed (of temperature waves) in the cold water zone is

$$v^0 = \frac{C_w^p(T^0)}{C_r^p(T^0) + \varphi C_w^p(T^0)} u^0. \tag{46}$$

## 3 Wave bifurcation analysis

Let us consider the situation where the hot steam zone is followed by a cold water zone. For such a situation to occur, there must be a steam condensation discontinuity in between. Let us first examine the critical case (\*) when the speed of the condensation discontinuity is the same as the characteristic speed in the cold water zone.

### 3.1 The hot-cold bifurcation

Because speed equality of different waves typically represents resonance and generates bifurcations, let us consider the case when the SCF speed is so large that it equals the cooling contact discontinuity speed. We expect this bifurcation

to represent the boundary between configurations containing either  $SCF$  shocks or cooling discontinuities. Equating the cooling discontinuity speed  $v_w^{b,0}$  (from Eq. (33) or equivalently from (35)) with  $v^{SCF}$  given by Eq. (45). Using Eq. (26), we conclude that we have the following remarkable speed equalities.

**Theorem 1.** *Fix  $T^0$  and  $T^b$  (or equivalently  $T^0$  and the reservoir pressure). Consider the following three shocks: HISW shock between  $(S_w^b, T^b, u^b)$ ,  $(1, T^b, u^b)$ , cooling shock between  $(1, T^b, u^b)$ ,  $(1, T^0, u^0)$ ,  $SCF$  between  $(S_w^b, T^b, u^b)$ ,  $(S_w^0, T^0, u^0)$ , with speeds  $v_{g,w}^b$ ,  $v_w^{b,0}$  and  $v^{SCF}$  respectively. If any two of their wave speeds coincide at a certain  $S_w^b = S_*$ , then their three speeds coincide at this  $S_*$ .*

**Proof.** The proof consists of three parts. The velocities are given in Eqs. (26), (35) and (42).

(1) Assume that at  $S_w^b = S_*$  we have  $v_{g,w}^b = v_w^{b,0}$ .

From the equality in speeds, Eqs. (26) and Eqs. (33) we have for  $S_g^b = 1 - S_*$ :

$$\frac{u^b f_g^b}{\varphi S_g^b} = \frac{u^b (1 - f_w^b)}{\varphi (1 - S_w^b)} = u^b \frac{H_w^b}{H_r^b + \varphi H_w^b}. \quad (47)$$

Multiplying numerator and denominator of the second fraction in Eq. (47) by  $H_w^b$  and subtracting the results to the corresponding terms in the third fraction, we obtain:

$$\frac{u^b f_g^b}{\varphi S_g^b} = u^b \frac{H_w^b f_w^b}{H_r^b + \varphi H_w^b S_w^b}. \quad (48)$$

Multiplying numerator and denominator of the first fraction in Eq. (48) by  $H_g^B$  and adding the results to the corresponding terms in the second equation, we obtain:

$$\frac{u^b f_g^b}{\varphi S_g^b} = u^b \frac{H_w^b f_w^b + H_g^B f_g^b}{H_r^b + \varphi H_w^b S_w^b + \varphi H_g^B S_g^b}. \quad (49)$$

From Eqs. (26) and (42), we see that  $v_{g,w}^b = v^{SCF}$ .

- (2) Performing the above calculation in reverse order, we can prove that  $v_{g,w}^b = v^{SCF}$  implies  $v_{g,w}^b = v^{SCF} = v_w^{b,0}$ .
- (3) Assume that at  $S_*$  we have  $v_w^{b,0} = v^{SCF}$ .

From Eqs. (35) and (42), and assuming that  $\rho_w^b = \rho_w^0$ , i.e. the density of water is independent of temperature,

$$v_w^{b,0} = u^b \frac{H_w^b}{H_r^b + \varphi H_w^b} = u^b \frac{H_w^b f_g^b + H_g^B f_g^b}{H_r^b + \varphi H_w^b S_w^b + \varphi H_g^B S_g^b}. \tag{50}$$

Substituting  $f_w^b = 1 - f_g^b$ ,  $S_w^b = 1 - S_g^b$  in the numerator and denominator of the last fraction in Eq. (50) we obtain:

$$v_w^{b,0} = u^b \frac{H_w^b}{H_r^b + \varphi H_w^b} = u^b \frac{H_w^b - H_w^b f_g^b + H_g^B f_g^b}{H_r^b + \varphi H_w^b - \varphi H_w^b S_g^b + \varphi H_g^B S_g^b}. \tag{51}$$

Subtracting the numerator and denominator of the first fraction from the corresponding terms in the last fraction we obtain:

$$v_w^{b,0} = \frac{u^b f_g^b (-H_w^b + H_g^B)}{\varphi S_g^b (-H_w^b + H_g^B)}, \tag{52}$$

or, from Eq. (26),  $v_w^{b,0} = v_{g,w}^b$ , and the proof is complete. □

The speed  $v_{g,w}^b$  is the Buckley-Leverett speed of propagation of a hot steam shock from  $S_w^b$  to  $S_w = 1$  (pure hot water, or no steam) governed by Eq. (24). Thus, each pair of states of this one-parameter family of discontinuities  $(S_*, T^b, u^b)$ ,  $(1, T^0, u^0)$  acts as an organizing center in the space of all solutions of the Riemann problem; the first member  $(S_*, T^b, u^b)$  of each such pair is denoted by  $*$ . This family of discontinuities is parameterized by  $u^0$  for instance, as explained in Remark 2.

Theorem 1 provides information related to the structure at the left of the temperature discontinuities. In Figure 3,  $S_*$  corresponds to the saturation of a state  $*$ . See also Figure 4. The  $*$  state separates two different configurations; in one of them, there is a hot steam zone and a cold water zone separated by a *SCF*, while in the other there is a hot steam zone, a hot water zone and a cold water zone.

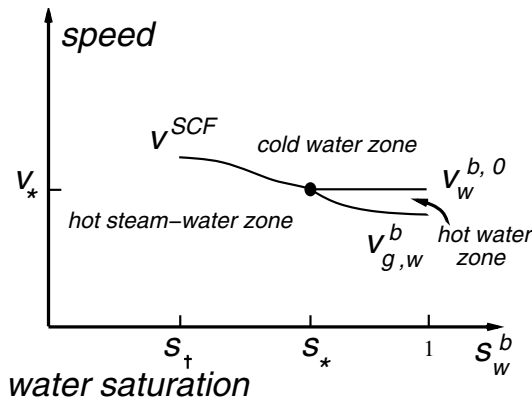


Figure 3 – Schematic bifurcation diagram near  $S_*$  (for fixed  $u^0, T^0$ ) versus  $S_w^b$ , the saturation on the left of the *HISW* shock or of the *SCF*.

### 3.2 The steam-water bifurcation

Let us fix  $T^0$  and  $T^b$  (or equivalently  $T^0$  and the reservoir pressure). Let us now examine the critical case ( $\dagger$ ) when the speed of the steam condensation discontinuity is so high that it becomes the same as the characteristic speed of saturation waves in the hot region given in Eq. (25), so the *SCF* overtakes the cooling discontinuity. One can expect that the *SCF* cannot exist with higher speed. At  $S_{\dagger}$ , the *SCF* becomes a left-contact. At such a state  $(S, T, u) = (S_{\dagger}, T^b, u^b)$ , we have:

$$v_s^b(S_{\dagger}; u^b) \equiv \frac{u^b}{\varphi} \frac{\partial f_w^b}{\partial S_w}(S_{\dagger}) = v^{SCF}. \tag{53}$$

It is easy to find numerically or graphically (see Fig. 5) the solution of Eq. (53) using Eq. (42) and solve for  $S_{\dagger}$ . Notice that  $u^b$  cancels out. Subsequently we can use Equation (44) to calculate the downstream velocity  $u^0$  in terms of  $v^{SCF}$ . Equivalently, we can use Eqs. (44), (45) to obtain  $u^b$  and  $v^{SCF}$  in terms of  $u^0$ .

**Remark 10.** If Figure 5 were drawn to scale for the actual data nothing would be visible. The drawing is for illustrative purposes. In the numerical example studied in detail, we find the following values:  $S^{\dagger} = -1.32449$ ,  $f^{\dagger} = -0.00471$ ,  $S^{infl} = 0.884747$ ,  $S_{\dagger} = 0.308042$ ,  $S_{\dagger\dagger} = 0.991435$ , and  $S_* = 0.983167$ .

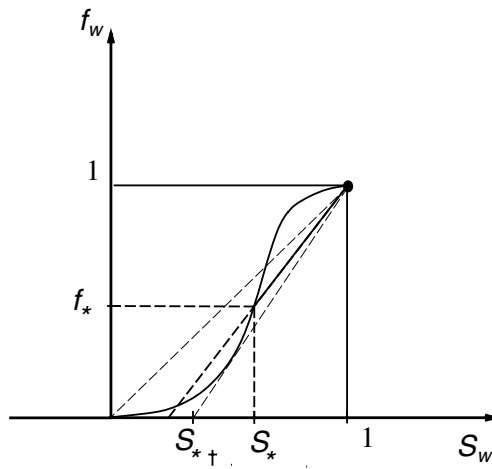


Figure 4 – Finding  $S_*$  from second equality in Eq. (47), by a solid line with slope  $\varphi H_w^b / (H_r^b + \varphi H_w^b)$ ; dashed bounding lines through  $(0, 0)$  and  $(S_{*+}, 0)$ .

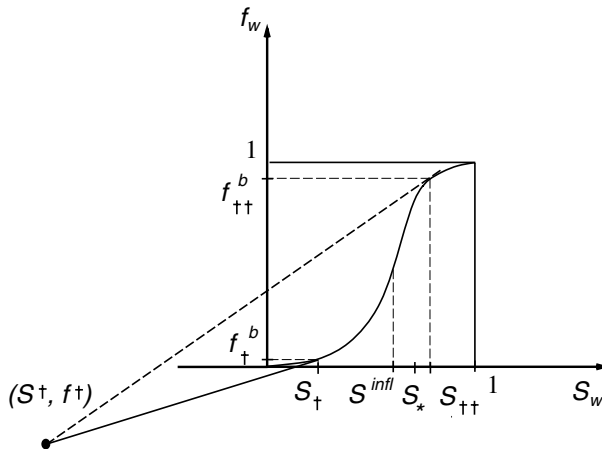


Figure 5 – Graphical solution of Eqs. (53) and (42) for steam-water bifurcation. See Eq. (54). The solid line represents the  $SCF$  shock.

Equating  $v^{SCF}$  given by Eq. (53) with Eq. (42), making  $f_g^b = 1 - f_w^b$ ,  $S_g = 1 - S_w$ , we obtain

$$\frac{\partial f_w^b}{\partial S_w}(S_{*+}) = \frac{f_w^b(S_{*+}) - f_{*+}^b}{S_{*+} - S_{*+}^b}, \tag{54}$$

where

$$S^\dagger = \frac{H_r^b / \varphi + H_g^B}{H_g^B - H_w^b}, \quad f^\dagger = \frac{H_g^B}{H_g^B - H_w^b}, \quad (55)$$

and all quantities are evaluated at the boiling temperature  $T^b$ . The physics of water at normal pressure dictates that at the boiling temperature,  $H_g^B < H_w^b$ , thus  $S^\dagger < 0$  and

$$f^\dagger < 0. \quad (56)$$

**Remark 11.** Since for steam–water  $(S^\dagger, T^\dagger)$  satisfies the inequalities (56), there is another solution point  $(S_{\dagger\dagger}, f_{\dagger\dagger}^b)$  for Eq. (53) closer to (1,1) as shown in Fig. 5. However, it does not play any role in the Riemann solution of the current problem because it exceeds  $S_*$ , according to Remark 10.

The contact bifurcation  $S_\dagger$  separates different wave structures in the steam-water zone as can be seen in Fig. 6.

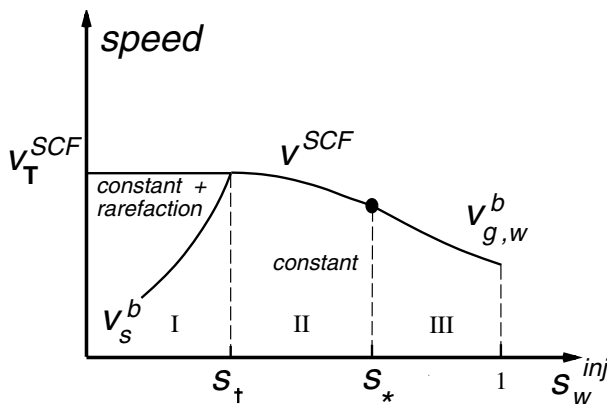


Figure 6 – Structure of the steam-water zone below solid curve marked by  $v_s^b, v_T^{SCF}, v^{SCF}, v_{g,w}^b$  given in Eqs. (25), (42) with  $S_w = S_\dagger$ , Eq. (42) with  $S_\dagger < S_w^{inj} < S_*$ , and Eq. (26) respectively. The figure is not drawn to scale.

In Figures 11 and 2, we show the characteristic speed  $v^{SCF}$  and  $u^b$  for each  $S_w^b$ , at temperature  $T^b$  for fixed  $u^0$ . As we shall see in Section 4.2, the diagram in Fig. 11 determines the structure of the Riemann solution in the steam zone.

**Remark 12.** By inspection of Figure 5, we see that slightly above  $S_{\dagger}$  there exist  $S_+$  and slightly below  $S_{\dagger}$  there exist  $S_-$ , such that in the limit as  $S_+ = S_-$  we have  $v^{SCF}(S_+) = v^{SCF}(S_-)$  larger than  $v^{SCF}(S_{\dagger})$ , satisfying as well

$$\begin{aligned} (S_+ - S_{\dagger})v^{SCF}(S_+) &= \frac{u^b}{\varphi}(f_w^b(S_+) - f_{\dagger}) \\ (S_- - S_{\dagger})v^{SCF}(S_-) &= \frac{u^b}{\varphi}(f_w^b(S_-) - f_{\dagger}) \end{aligned}$$

Subtracting these two equations, dividing by  $(S_+ - S_-)$  and taking the limit as  $S_+, S_- \rightarrow S_{\dagger}$  we recover that

$$\frac{u^b}{\varphi} \frac{\partial f_w^b}{\partial S_w}(S_{\dagger}) = v^{SCF}, \tag{59}$$

and obtain that  $S_{\dagger}$  maximizes  $v^{SCF}$ , as illustrated in Figures 3, 6 and 11. An analogous argument holds at  $S_{\dagger\dagger}$ .

**Remark 13.** The *SCF* shocks are represented in Figure 5 as segments with slope  $(v^{SCF}/u^b)$  between  $(S^{\dagger}, f^{\dagger})$  and  $(S, f)$  for  $0 \leq S \leq S_{\dagger}$ . We see that as  $S$  increases  $v^{SCF}$  decreases and the shock amplitude  $S - S^{\dagger}$  increases.

**Remark 14.** We have shown that  $(v^{SCF}/u^b)$  has an extremum at  $S_{\dagger}$ ; the Figure 5 shows that this slope has an extremum at  $S_{\dagger\dagger}$ . Thus  $(v^{SCF}/u^b)$  also has an extremum at  $S_{\dagger\dagger}$ .

### 3.3 Waves in the liquid water region

Because the initial reservoir temperature is  $T^0$ , the liquid water region must always contain a cold water zone at temperature  $T^0$  far away from the place where hot steam is injected. If the liquid water region receives water at temperature  $T^b$  from the steam zone, the liquid water region consists of a hot liquid water zone at temperature  $T^b$  and a cold water zone at temperature  $T^0$ , separated by a cooling discontinuity that moves with speed  $v_w^{b,0}$  given by Eq. (35). This cooling discontinuity exists provided  $v_w^{b,0} > v_{g,w}^b$  from Eq. (26) i.e. the hot isothermal steam-water shock velocity (*HISW*). In this case the *HISW* shock at which

the steam saturation becomes zero and the cooling shock where the temperature jumps to the ambient temperature are separated. See region  $S > S_*$  in Fig. 3.

On the other hand, if  $v_w^{b,0} > v_{g,w}^b$  were to be violated, there would be no hot water zone and no cooling discontinuity. See region  $S < S_*$  in Fig. 3, where there is a steam condensation front instead of a cooling discontinuity.

### 3.4 Waves in the hot steam zone

The waves in this zone can be found by a pure Buckley-Leverett or Oleńnik analysis of Eq. (24), with one *caveat*. In the sequence of zones starting at the injection well, the first zone is a steam zone, and the last one is a cold water zone, with heat flow governed by the system (29)–(30). The cold water zone is reached either via a steam condensation shock or via a cooling shock. In the latter case, if there is no other shock between the steam zone and the cold water zone, all waves in the steam zone must have speeds that do not exceed the cooling shock speed  $v_w^{b,0}$  given by Eq. (34). In particular, if there is a *HISW* shock with speed given by  $v_{g,w}^b$  in Eq. (26), we must have  $v_{g,w}^b \leq v_w^{b,0}$ . Similarly, if there is a saturation rarefaction wave with speed given by  $v_s^b$  in Eq. (25), we must have  $v_s^b \leq v_w^{b,0}$ , the cooling contact discontinuity velocity.

Because of Theorem 1, we see that the restrictions above are satisfied precisely for saturation  $S_w^b$  in the hot water zone with values between  $[S_*, 1]$ , see Figure 11. For steam–water at the conditions considered in this work, one can verify that the steam–water bifurcation water saturation  $S_{\dagger}$  is smaller than  $S_*$  in Fig. 5. Because  $S_{\dagger} < S_*$ , there are no Buckley-Leverett shocks between  $[S_{wc}, S_*]$ . This is so because below  $S_{\dagger}$  there are no shocks as rarefaction wave velocities increase monotonically from  $S_{wc}$  to  $S_{\dagger}$ . At  $S_{\dagger}$  the velocity is equal to the *SCF* velocity. Between  $S_{\dagger}$  and  $S_*$  there are no shocks as the rarefaction wave velocities are larger than the *SCF* velocity.

Another case of interest occurs if pure steam is injected, *i.e.*  $S_w = S_{wc}$ , the connate water saturation. In this case, a saturation rarefaction wave starts at  $x = 0$  in the steam zone. A mixture of steam and water can also be injected. As long as  $S_w^{inj} < S_{\dagger}$ , at  $x = 0$  there is a constant state followed by a saturation rarefaction wave. Of course, in the Buckley-Leverett solution for the steam zone the rarefaction wave containing a saturation value  $S_w$  satisfies the geometric

compatibility condition:

$$\frac{u^{inj}}{\varphi} \frac{\partial f_w^b(S_w)}{\partial S_w} \leq v^{SCF}. \tag{60}$$

### 4 Construction of the Riemann solution

Here we describe a systematic way of constructing the Riemann solution through a *wave curve*. Then we summarize the resulting Riemann solution.

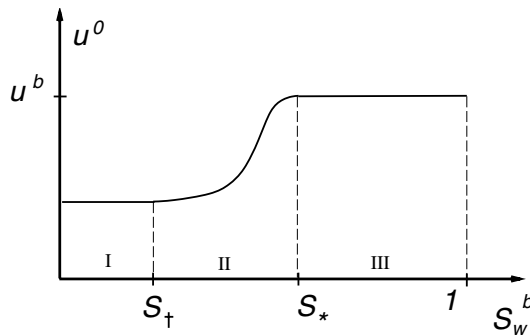


Figure 7 – Speed  $u^0$  for fixed  $T^b, u^{inj}$ , obtained from Eq. (7) and Fig. 2.

#### 4.1 The wave curve

Let us fix the initial state of the reservoir as  $S_w^0 = 1, T = T^0, u = u^0$ , which is necessarily the rightmost constant state in the Riemann solution. It turns out to be convenient for the discussion to imagine that an arbitrary value for  $u_0$  has been specified. Let us decrease the injection saturation  $S_w^{inj}$  (at the boiling temperature) from  $S_w = 1$  to  $S_w = S_{wc}$ ; in our case this corresponds to changing  $S_w^b$ , the water saturation at the *HISW* shock with speed given in Eq. (26). For each  $S_w^{inj}$ , we construct the sequence of elementary waves (and constant states) with decreasing speeds from right to left, that is from  $S_w^0$  to  $S_w^b$ . There is a constant state to the left of  $S_w^b$ , so there is no other wave to the left of  $S_w^b$ , the steam shock. For each  $S_w^b$ , we mark its wave speed, forming the solid curves in Fig. 11. This sequence, parameterized by  $S_w^b$ , is called a *backward wave curve* from  $(S_w = 1, T^0, u^0)$ . It combines all information needed for describing the structure of the Riemann solution, and for verifying necessary speed relations for the admissibility of the

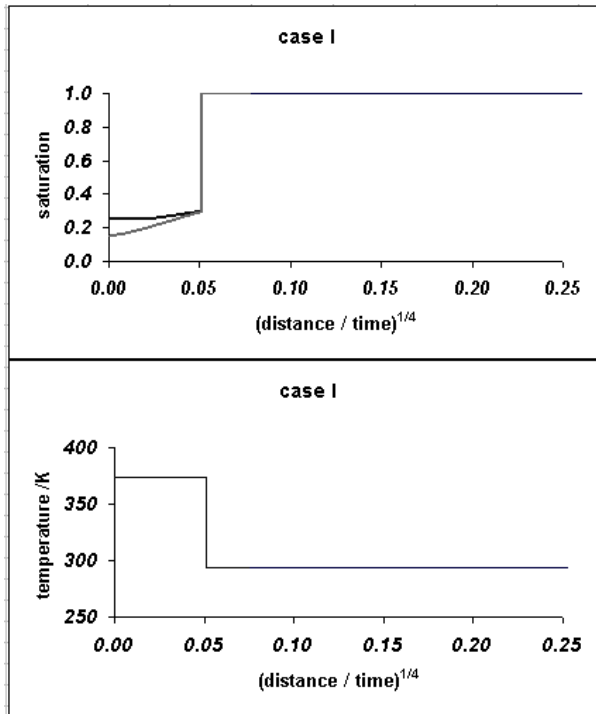


Figure 8 – Two cases of steam injection: at connate water saturation  $S_{wc}$  or at a low water saturation. With injection at  $S_{wc}$  there is a rarefaction wave and a  $SCF$ . With injection of low water saturation above  $S_{wc}$  there is a constant state before the rarefaction.

shocks involved. On rarefaction segments of this backward wave curve, the characteristic speed decreases, while on shock segments of this wave curve, the shock speed increases [8], [14]. We refer to Fig. 11.

When  $S_w^{inj}$  lies between  $S_*$  and 1, the wave with fastest possible speed is the cooling shock in the liquid water region (see Section 3.4), so the backward wave curve corresponds to such a shock wave, with speed given by  $v_w^{b,0}$  in Eq. (35). There is a hot steam-water region and a cold water zone. In the hot steam-water region, generically there is a Buckley-Leverett rarefaction-shock and a constant state. The hot steam-water region terminates with the  $HISW$  shock.

The analysis from now on relies on the fact that for steam–water in the actual reservoir,  $S^{infl} < S_*$ . For  $S_w^{inj}$  within  $(S_†, S_*)$ , the wave with slowest speed is the  $SCF$ , with speed  $v^{SCF}$ . At the left of the  $SCF$ , characteristic speed  $v_s^b$  exceeds

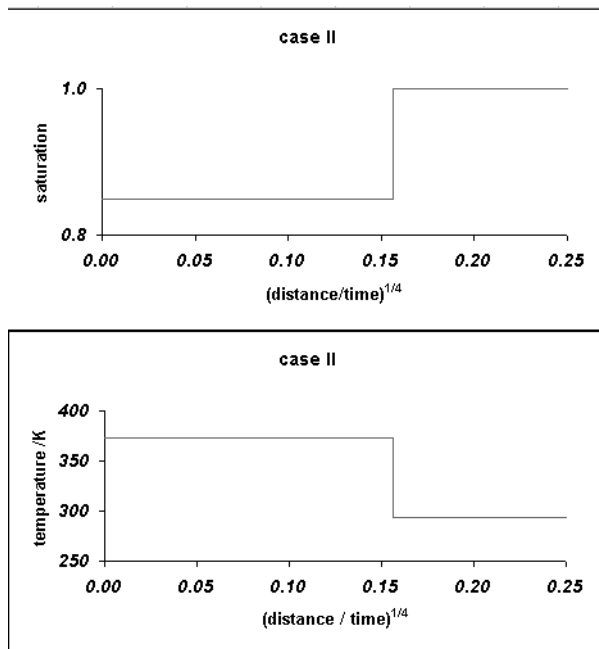


Figure 9 – Steam injection at intermediate water saturation. We get a constant state upstream and the steam condensation front. The  $SCF$  moves faster than in Figure 8.

$v^{SCF}$ , so there can be no rarefactions nor shocks to the left of the  $SCF$ . Thus, for  $S_w^{inj}$  in such range, the solution (from left to right) consists of a constant state of steam and water at temperature  $T^b$ , a  $SCF$  jumping from  $S_w^{inj}$  to 1.0, and a constant cold water zone.

Recall that  $S_{\dagger} < S_w^{infl}$ . Therefore, from  $S_w^{inj}$  within  $(S_{wc}, S_{\dagger})$ , the slowest speed is a hot steam–water rarefaction speed  $v_s^b$ , which is smaller than  $v^{SCF}$  ( $v_s^b$  and  $v^{SCF}$  coincide at the left state  $S_{\dagger}$ ), so there are rarefactions to the left of the  $SCF$ . Thus the solution consists of a constant state with saturation  $S_w^{inj}$  as in the previous case (this constant state disappears if  $S_w^{inj} = S_{wc}$ ), a rarefaction wave from  $S_w^{inj}$  to  $S_{\dagger}$ , a  $SCF$  from  $S_{\dagger}$  to 1, and a constant cold water zone.

Let us explain how the Darcy velocity  $u^b$  is constructed for each value of  $S_w^{inj}$ . If  $S_w^{inj}$  lies in the interval  $(S_*, 1)$ ,  $u^b$  is given by Eq. (34), and the speed  $v_w^{b,0}$  of the cooling shock is given by Eq. (35) (Case III). (As explained in Section 2.1, the velocity  $u$  is constant in the hot region and equals  $u^b$ .) If  $S_w^{inj}$  lies in the

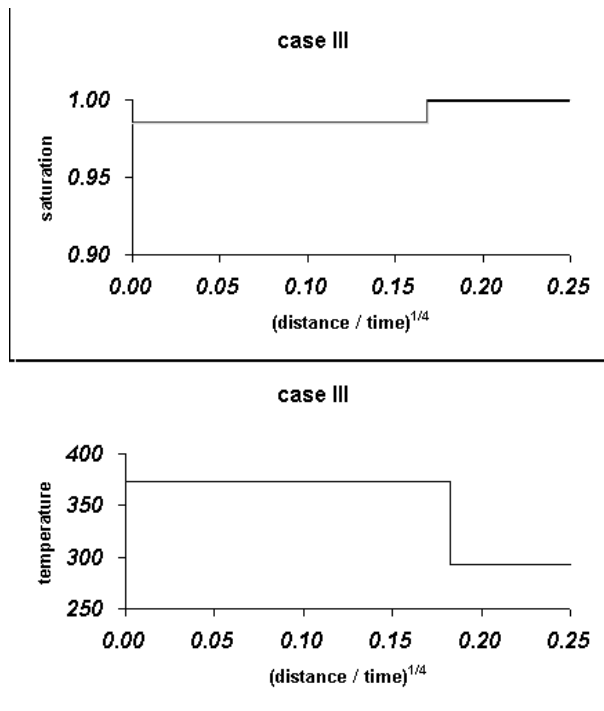


Figure 10 – Steam injection at a high water saturation. We get a constant state upstream, the Buckley-Leverett-saturation shock and the cooling discontinuity. These two waves have distinct speeds; they are both faster than the *SCF* in Figure 9.

interval  $S_{\dagger}$  and  $S_*$ ,  $u^b$  is given by Eq. (44). The speed of the *SCF* is given by Eq. (45), (Case II).

If  $S_w^{inj}$  lies in the interval  $(S_{wc}, S_{\dagger})$  (Case I, since  $u^b$  has to match at the boundary of Cases I and II,  $u^b$  is given by Eq. (45) with  $S_w$  replaced by  $S_{\dagger}$ . Thus  $u^b$  is independent of  $S_w^{inj}$  in Case I.

A summary of the behavior of  $u^b(S_w^{inj})$  is presented in Fig. 2. Here  $u^b(S_w^{inj})$  is the value of  $u^b$  calculated in the previous paragraphs for a fixed  $u^0$ .

We are ready to abandon the assumption that  $u^0$  is known. This is impractical, since normally one specifies  $u^{inj}$  rather than  $u^0$ . We take advantage of the fact that all speeds are proportional to find the actual speed in the cold water zone

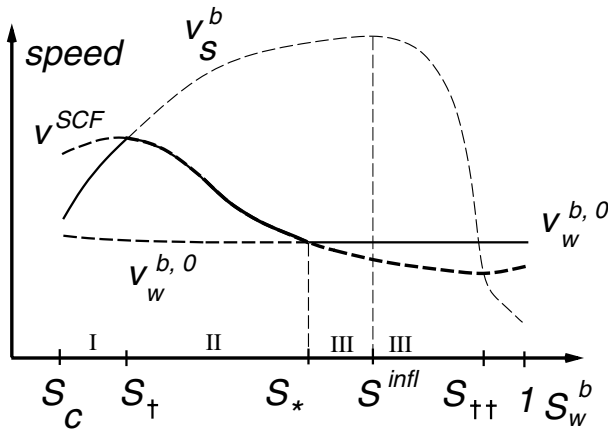


Figure 11 – Wave speed diagram for left states  $(S_w^b, T^b, u^b)$  reachable from the right state  $(1, T^0, u^0)$ ; for this right state the curve marked  $v^{SCF}$  is the Rankine-Hugoniot curve projected onto the  $(S_w, v)$  plane. The velocity of the SCF is  $v^{SCF}$  (Eq. (42)),  $v_s^b$  is the hot region saturation characteristic speed (Eq. (25)), and  $v_w^{b,0}$  is the velocity of the cooling contact discontinuity (Eq. (35)).

$u^0(S_w^{inj})$  for specified  $u^{inj}$ , as follows:

$$\frac{u^b(S_w^{inj})}{u^0} = \frac{u^{inj}}{u^0(S_w^{inj})}. \tag{61}$$

From this equation we recover  $u^0(S_w^{inj})$ , essentially by inverting the variable represented in the ordinate in Fig. 2. Thus we obtain Fig. 7.

#### 4.2 Summary of the Riemann solution

The solution consists of three parts, viz. a hot region (A) at constant boiling temperature, an infinitesimally thin cooling front (B) or discontinuity, where all possible steam condensation occurs, and a cold liquid water region downstream (C). See Figure 1.

As we have seen, the nature of the solution changes and there are three possible cases (I), (II), and (III), depending on the injected steam quality  $S_g^{inj} = 1 - S_w^{inj}$ . Cases (II) and (III) are separated by the hot-cold bifurcation, while Cases (I) and (II) are separated by the steam-water bifurcation.

Case (I) occurs when the saturation wave velocity  $v_s^b(S_w^{inj}; u^{inj}) \leq v^{SCF}$  (see Eq. (25)); it consists of a sequence of a constant state at the injection end, a rarefaction wave in the hot steam zone (A) ending with saturation  $S_{\dagger}$  at the SCF (B) with speed  $v^{SCF}$  defined by saturations  $S_{\dagger}$  and  $S_w = 1$ , and a cold water constant state in (C). The constant state in (A) disappears if the injection saturation is  $S_{wc}$ , that is, pure steam is injected. See Fig. 8. The rarefaction disappears for  $v_s^b(S_w^{inj}; u^{inj}) = v^{SCF}$ , as in this case  $S_w^{inj} = S_{\dagger}$ .

Case (II) occurs for  $v_{g,w}^b(S_w^{inj}, u^{inj}) < v^{SCF} < v_s^b(S_w^{inj}; u^{inj})$ ; see Eqs. (25), (26) and (27). This case consists of a hot constant steam–water state in (A), the SCF (B) with speed  $v^{SCF}$  defined by left and right saturations  $S_w^{inj}$  and 1 (see Eq. (45)), and a constant cold water state in (C). See Fig. 9.

Case (III) occurs for a typically small region for the cooling contact discontinuity velocity  $v_w^{b,0}$  (given in Eq. (35)) with  $v_w^{b,0} > v_{g,w}^b(S_w^{inj}, u^{inj})$  (see Eq. (26)), i.e. the hot isothermal steam–water shock velocity. In this case, there is no SCF. In the hot region (A) there is a constant state with steam–water, then another constant state of pure hot water at the same boiling temperature, separated by a Buckley–Leverett shock. Then there is a cooling shock with speed  $v_w^{b,0}$ , where the saturation of water is constant ( $S_w = 1$ ) and the temperature changes from  $T^b$  to the reservoir temperature  $T^0$ . (See Fig. 10.)

Figure 6 illustrates the saturation dependence of the various velocities that are the basis of the steam–water zone structure, for Cases (I), (II), (III).

## 5 Lax conditions for the steam condensation front

Despite the fact that our system does not satisfy Lax’s theorem hypotheses, we will compare the SCF speed to the left and right characteristic speeds. We will conclude that from the point of view of Lax’s inequalities, the SCF is a 2-shock or a limit of such shocks.

We introduce the heat capacities  $C_p(T)$  as the temperature derivatives of the enthalpies [J/m<sup>3</sup>] at constant pressure, i.e.  $C_w^p(T)$  is the heat capacity of water and  $C_g^p(T)$  is the heat capacity of steam. In the same way we define the thermal expansivity of water and steam  $\alpha_w(T)$  and  $\alpha_g(T)$  as minus the temperature derivative of the density divided by the density (see Appendix A).

Eqs. (21)–(22) may be written in quasilinear form as:

$$\begin{aligned}
 -\frac{\partial u}{\partial x}(\rho_w f_w + \rho_g f_g) &= -\varphi \left[ (S_w \rho_w \alpha_w + S_g \rho_g \alpha_g) \frac{\partial T}{\partial t} \right. \\
 &+ \left. (\rho_g - \rho_w) \frac{\partial S_w}{\partial t} \right] - u \left[ (f_w \rho_w \alpha_w + f_g \rho_g \alpha_g \right. \\
 &+ \left. (\rho_g - \rho_w) \partial f_w / \partial T) \frac{\partial T}{\partial x} - \left( (\rho_w - \rho_g) \frac{\partial f_w}{\partial S_w} \right) \frac{\partial S_w}{\partial x} \right],
 \end{aligned} \tag{62}$$

$$\begin{aligned}
 q \Lambda^0 - \frac{\partial u}{\partial x} (H_w f_w + H_g^s f_g) &= \varphi \left[ \left( \frac{C_r^p}{\varphi} + S_w C_w^p + S_g C_g^p \right) \frac{\partial T}{\partial t} \right. \\
 &+ \left. (H_w - H_g^s) \frac{\partial S_w}{\partial t} \right] + u \left[ (f_w C_w^p + f_g C_g^p \right. \\
 &+ \left. (H_w - H_g^s) \partial f_w / \partial T) \frac{\partial T}{\partial x} + \left( (H_w - H_g^s) \frac{\partial f_w}{\partial S_w} \right) \frac{\partial S_w}{\partial x} \right].
 \end{aligned} \tag{63}$$

We restrict our attention to regions where  $\partial u / \partial x = 0$  and  $q = 0$ , that is, away from any kind of shocks. Thus, the LHS terms of Eqs. (62), (63) vanish.

We let

$$\begin{aligned}
 A_I &= \frac{C_r^p}{\varphi} + S_w C_w^p + S_g C_g^p, \\
 A_{II} &= f_w C_w^p + f_g C_g^p + (H_w - H_g^s) \partial f_w / \partial T.
 \end{aligned} \tag{64}$$

Multiplying the RHS of Eq. (62) by  $-(H_w - H_g^s)$  and of Eq. (63) by  $(\rho_w - \rho_g)$  and adding leads to a new equation, which will be used instead of Eq. (63):

$$\begin{aligned}
 \varphi \left[ (H_w - H_g^s) (S_w \rho_w \alpha_w + S_g \rho_g \alpha_g) + (\rho_w - \rho_g) A_I \right] \frac{\partial T}{\partial t} \\
 + u \left[ (H_w - H_g^s) \left( f_w \rho_w \alpha_w + f_g \rho_g \alpha_g + (\rho_g - \rho_w) \partial f_w / \partial T \right) \right. \\
 \left. + (\rho_w - \rho_g) A_{II} \right] \frac{\partial T}{\partial x} = 0.
 \end{aligned} \tag{65}$$

We let

$$A_{III} = (H_w - H_g^s) (S_w \rho_w \alpha_w + S_g \rho_g \alpha_g) + (\rho_w - \rho_g) A_I, \tag{66}$$

$$A_{IV} = \left( (H_w - H_g^s) (f_w \rho_w \alpha_w + f_g \rho_g \alpha_g + (\rho_g - \rho_w) \partial f_w / \partial T) \right. \\ \left. + (\rho_w - \rho_g) A_{II} \right). \quad (67)$$

Thus in regions where  $\partial u / \partial x = 0$  and  $q = 0$ , that is, away from any kind of shocks (see Remarks 1 and 2), Eqs. (62)–(65) may be written in matrix form as:

$$\left( A \frac{\partial}{\partial t} + B \frac{\partial}{\partial x} \right) \begin{pmatrix} S \\ T \end{pmatrix} = 0. \quad (68)$$

Let  $\mu$  be a characteristic speed. Then the determinant of the following matrix must vanish:

$$-\mu \varphi \begin{pmatrix} (\rho_g - \rho_w) & (S_w \rho_w \alpha_w + S_g \rho_g \alpha_g) \\ 0 & A_{III} \end{pmatrix} \\ + u \begin{pmatrix} (\rho_g - \rho_w) \partial f_w / \partial S_w & f_w \rho_w \alpha_w + f_g \rho_g \alpha_g + (\rho_g - \rho_w) (\partial f_w / \partial T) \\ 0 & A_{IV} \end{pmatrix}. \quad (69)$$

Since the matrix above is upper triangular, the characteristic speeds are easily read from the diagonals:

$$\mu = \frac{u}{\varphi} \frac{\partial f_w}{\partial S_w} \quad \text{and} \quad \mu = \frac{u}{\varphi} \frac{A_{IV}}{A_{III}}. \quad (70)$$

(It is easy to check that  $A_{III}$  never vanishes.)

Now, in the liquid water region on the right of the *SCF*,  $S_g = 0$ ,  $f_g = 0$ ,  $\frac{\partial f_w}{\partial S_w} = 0$ , the characteristic speeds are

$$\mu = 0 \quad \text{and} \quad v^0 = \frac{C_w^p(T^0)}{C_r^p(T^0) + \varphi C_w^p(T^0)} u^0. \quad (71)$$

The latter speed has already been calculated in Eq. (46).

On the other hand, in the hot steam zone the characteristic speeds are

$$v_s^b = \frac{u^b}{\varphi} \frac{\partial f_w^b}{\partial S_w}, \quad \text{and} \quad v_T^b = \frac{u^b}{\varphi} \frac{A_{IV}(T^b)}{A_{III}(T^b)}. \quad (72)$$

The first speed has already been calculated in Eq. (45). The second speed of thermal waves is shown in Figure 11 as a function of  $S_w$  at  $T = T^b$ .

For a  $(-)$  state for the  $SCF$  with  $S_w$  in  $(S_*, S_†)$  we have that the thermal characteristic speed in the steam zone satisfies  $0 < v^0 < v^{SCF}$ , and the steamfront velocity satisfies  $v_T^b < v^{SCF} < v_s^b$ , so the  $SCF$  would be called a 2-shock in Lax's classification scheme. However, Lax's theorem only applies to shocks with small amplitude, while the  $SCF$  is a large shock, and only if the governing equations were a system of conservation laws satisfying appropriate technical hypotheses, such as genuine nonlinearity, which is actually violated at the inflection  $S^{infl}$ . Moreover, even the Lax inequalities are violated starting at the steam-water bifurcation; there is no conclusive mathematical evidence that the  $SCF$  shock needed to complete the Riemann solution is physically admissible. This is the issue left open.

## 6 Summary and conclusions

A complete and systematic description of all possible solutions of the Riemann problem for the injection of a mixture of steam and water into a water-saturated porous medium, for all possible reservoir temperatures and pressures below the water critical point. For each Riemann data, we found a unique solution.

As determined by the dissipative effects of capillary porous forces combined with the mass source term given in Eq. 3, the internal structure of the  $SCF$  is consistent with the Riemann solution in this work. This fact is demonstrated in a companion paper [4].

## 7 Acknowledgments

This work was partially done at IMA, University of Minnesota, and therefore partially funded by NSF. H.B. thanks Shell for the continuous support of the steam drive recovery research at the Delft University of Technology. We also thank Beata Gundelach for careful and expert typesetting of this paper. We thank the referees for suggestions that improved the paper.

## Appendix A – Physical quantities; symbols and values

In this Appendix we summarize the values and units of the various quantities used in the computation and empirical expressions for the various parameter

<i>Physical quantity</i>	<i>Symbol</i>	<i>Value</i>	<i>Unit</i>
Water, steam fractional functions	$f_w, f_g$	Eq. (9).	$[\text{m}^3/\text{m}^3]$
Water-steam frac. flow, hot region	$f_w^b, f_g^b$		$[\text{m}^3/(\text{m}^2\text{s})]$
Porous rock permeability	$k$	$1.0 \times 10^{-12}$	$[\text{m}^2]$
Water, steam relative permeabilities	$k_{rw}, k_{rg}$	Eq. (82), (82).	[-]
Pressure	$p$	$1.0135 \times 10^5$	[Pa]
Mass condensation rate	$q$	Eq. (3).	$[\text{kg}/(\text{m}^3\text{s})]$
Mass condensation rate coefficient	$q_b$	0.01	$[\text{kg}/(\text{m}^3\text{sK})]$
Steam injection rate	$u^{inj}$	$9.52 \times 10^{-4}$	$[\text{m}^3/(\text{m}^2\text{s})]$
Water, steam phase velocity	$u_w, u_g$	Eq. (2).	$[\text{m}^3/(\text{m}^2\text{s})]$
Total Darcy velocity	$u$	$u_w + u_g$ , Eq. (13).	$[\text{m}^3/(\text{m}^2\text{s})]$
Flow rate in hot region	$u^b$	Eq. (24), (34).	$[\text{m}^3/(\text{m}^2\text{s})]$
Flow rate in cold water zone	$u^0$	Eq. (31).	$[\text{m}^3/(\text{m}^2\text{s})]$
SCF velocity	$v^{SCF}$	Eq. (42).	[m/s]
Cooling contact disc. speed, hot water zone	$v_w^b$	Eq. (36).	[m/s]
Thermal characteristic speed, cold water zone	$v^0$	Eq. (46).	[m/s]
Saturation characteristic speed, hot region	$v_s^b$	Eq. (25).	[m/s]
Hot isothermal steam-water shock velocity	$v_{g,w}^b$	Eq. (26).	[m/s]
Cooling contact discontinuity velocity	$v_w^{b,0}$	Eq. (35).	[m/s]
Water, steam heat capacity *	$C_w^p, C_g^p$	$dH_w/dT, dH_g^s/dT$	$[\text{J}/(\text{m}^3\text{K})]$
Effective rock heat capacity	$C_r^p$	$2.029 \times 10^6$	$[\text{J}/(\text{m}^3\text{K})]$
Steam enthalpy	$H_g$	$\rho_g(T)(h_g(T) - h_w(T^0))$	$[\text{J}/\text{m}^3]$
Steam sensible heat	$H_g^s$	Eq. (77).	$[\text{J}/\text{m}^3]$
Steam latent heat	$H_g^l$	$\rho_g(T)\Lambda^0$	$[\text{J}/\text{m}^3]$
Rock enthalpy	$H_r$	$\rho_r C_r^p (T - T^0)$	$[\text{J}/\text{m}^3]$
Water enthalpy	$H_w$	$\rho_w(T)(h_w(T) - h_w(T^0))$	$[\text{J}/\text{m}^3]$
Water, rock enthalpy at boiling temperature	$H_w^b, H_r^b$	$H_w(T^b), H_r(T^b)$	$[\text{J}/\text{m}^3]$
Steam total, sensible enthalpy at boil. temp.	$H_g^B, H_g^b$	Eq. 43.	$[\text{J}/\text{m}^3]$

Table 2 – Summary of physical input parameters and variables.

<i>Physical quantity</i>	<i>Symbol</i>	<i>Value</i>	<i>Unit</i>
Water, rock enthalpy, reservoir temperature	$H_w^0, H_r^0$	$H_w(T^0), H_r(T^0)$	[J/m <sup>3</sup> ]
Water, steam saturations	$S_w, S_g$	Dependent variables.	[m <sup>3</sup> /m <sup>3</sup> ]
Connate water saturation	$S_{wc}$	0.15	[m <sup>3</sup> /m <sup>3</sup> ]
Water injection saturation	$S_w^{inj}$	See Section 4.	[m <sup>3</sup> /m <sup>3</sup> ]
Hot-cold bifurcation water saturation	$S_*$	Theorem 1.	[m <sup>3</sup> /m <sup>3</sup> ]
Steam-water bifurcation water saturation	$S_{\dagger}$	Eq. (53).	[m <sup>3</sup> /m <sup>3</sup> ]
Steam-water bifurcation ghost saturation	$S_{\dagger\dagger}$	See Remark 11.	[m <sup>3</sup> /m <sup>3</sup> ]
Water saturation at inflection	$S^{infl}$	Frac. flow infl. sat.	[m <sup>3</sup> /m <sup>3</sup> ]
Temperature	$T$	Dependent variable.	[K]
Reservoir temperature	$T^0$	293.	[K]
Boiling point of water–steam	$T^b$	Eq. (73).	[K]
Steam thermal expansion coefficient *	$\alpha_g$	$-(1/\rho_g)(\partial\rho_g/\partial T)_p$	[/K]
Water thermal expansion coefficient	$\alpha_w$	$-(1/\rho_w)(\partial\rho_w/\partial T)_p$	[/K]
Water, steam thermal conductivity	$\kappa_w, \kappa_g$	0.652, 0.0208	[W/(mK)]
Rock, composite thermal conductivity	$\kappa_r, \kappa$	1.83, Eq. (7).	[W/(mK)]
Saturation exponent for $P_c$	$\lambda_s$	0.5, Eq. (83)	[-]
Water, steam viscosity	$\mu_w, \mu_g$	Eq. (79), Eq. (78).	[Pa s]
Water, steam densities	$\rho_w, \rho_g$	Eq. (81), Eq. (80).	[kg/m <sup>3</sup> ]
Water, steam, rock densities – boiling temp.	$\rho_w^b, \rho_g^b, \rho_r^b$	Eq. (32)	[kg/m <sup>3</sup> ]
Water, steam, rock densities – reservoir temp.	$\rho_w^0, \rho_g^0, \rho_r^0$		[kg/m <sup>3</sup> ]
Interfacial tension	$\sigma_{wg}$	$58 \times 10^{-3}$	[N/m]
Rock porosity	$\varphi$	0.38	[m <sup>3</sup> /m <sup>3</sup> ]
Water evaporation heat at reservoir temperature	$\Lambda^0$	Eq. 1.	[J/kg]
Capillary diffusion coefficient	$\Omega$	Eqs. (11), (12).	[m <sup>3</sup> /m <sup>3</sup> ]

Table 2 – (continuation)

functions. For convenience we express the heat capacity of the rock  $C_r^p$  in terms of energy per unit volume of *porous medium* per unit temperature *i.e.* the factor  $1 - \varphi$  is already included in the rock density. All other densities are expressed in terms of mass per unit volume of the phase.

### A.1 Temperature dependent properties of steam and water

We use reference [16] to obtain all the temperature dependent properties below. The water and steam densities used to obtain the enthalpies are defined at the bottom. First we obtain the boiling point  $T^b$  at the given pressure  $p$ , *i.e.*

$$T^b = 280.034 + \ell(14.0856 + \ell(1.38075 + \ell(-0.101806 + 0.019017\ell))), \quad (73)$$

where  $\ell = \log(p)$  and  $p$  is the pressure in [k Pa]. The evaporation heat [J/kg] is given as a function of the temperature  $T$  at which the evaporation occurs. We use atmospheric pressure ( $p = 101.325$  [k Pa]) in our computations, to make the example representative of subsurface contaminant cleaning.

The liquid water enthalpy  $h_w(T)$  [J/kg] as a function of temperature is approximated by

$$\begin{aligned} h_w(T) = & 2.36652 \times 10^7 - 3.66232 \times 10^5 T + 2.26952 \times 10^3 T^2 \\ & - 7.30365 T^3 + 1.30241 \times 10^{-2} T^4 - 1.22103 \times 10^{-5} T^5 \\ & + 4.70878 \times 10^{-9} T^6. \end{aligned} \quad (74)$$

The steam enthalpy  $h_g$  [J/kg] as a function of temperature is approximated by

$$\begin{aligned} h_g = & -2.20269 \times 10^7 + 3.65317 \times 10^5 T - 2.25837 \times 10^3 T^2 \\ & + 7.3742 T^3 - 1.33437 \times 10^{-2} T^4 + 1.26913 \times 10^{-5} T^5 \\ & - 4.9688 \times 10^{-9} T^6. \end{aligned} \quad (75)$$

For the latent heat  $h_g^l$  [J/kg] or evaporation heat  $\Lambda(T)$  we obtain

$$\begin{aligned} h_g^l = & (7.1845 \times 10^{12} + 1.10486 \times 10^{10} T - 8.8405 \times 10^7 T^2 \\ & + 1.6256 \times 10^5 T^3 - 121.377 T^4)^{\frac{1}{2}}. \end{aligned} \quad (76)$$

The sensible heat of steam  $H_g^s(T)$  in [J/m<sup>3</sup>] is given as

$$H_g^s(T) = \rho_g (h_g(T) - h_w(T^0) - \Lambda(T^0)). \quad (77)$$

We also use the temperature dependent steam viscosity

$$\begin{aligned} \mu_g = & - 5.46807 \times 10^{-4} + 6.89490 \times 10^{-6}T - 3.39999 \times 10^{-8}T^2 \\ & + 8.29842 \times 10^{-11}T^3 - 9.97060 \times 10^{-14}T^4 \\ & + 4.71914 \times 10^{-17}T^5. \end{aligned} \tag{78}$$

The temperature dependent water viscosity  $\mu_w$  is approximated by

$$\begin{aligned} \mu_w = & - 0.0123274 + \frac{27.1038}{T} - \frac{23527.5}{T^2} + \frac{1.01425 \times 10^7}{T^3} \\ & - \frac{2.17342 \times 10^9}{T^4} + \frac{1.86935 \times 10^{11}}{T^5}. \end{aligned} \tag{79}$$

For the steam density as a function of temperature  $T[K]$  we use a different expression than [16] because our interest is a steam density at constant pressure, which is not necessarily in equilibrium with liquid water.

$$\rho_g(T) = p \frac{M_{H_2O}}{ZRT} \tag{80}$$

where  $p$  is the total pressure at which the steam displacement is carried out,  $R=8.31$  [J/mol K] and  $Z$  is the Z-factor (see e.g. Dake [6]) and  $M_{H_2O} = 0.018$  kg/mole is the molar weight of water. For the atmospheric pressures of interest here the Z-factor is close to unity. The liquid water density as a function of the temperature  $T[K]$  is given as

$$\begin{aligned} \rho_w(T) = & 3786.31 - 37.2487T + 0.196246T^2 - 5.04708 \times 10^{-4}T^3 \\ & + 6.29368 \times 10^{-7}T^4 - 3.08480 \times 10^{-10}T^5. \end{aligned} \tag{81}$$

### A.2 Constitutive relations

We use a porosity  $\varphi$  that is representative for unconsolidated sand. The relative permeability functions  $k_{rw}$  and  $k_{rg}$  are considered to be power functions of their respective effective saturations [7], *i.e.*

$$S_{we} = (S_w - S_{wc})/(1 - S_{wc}), \quad S_{ge} = S_g/(1 - S_{wc}).$$

The effective saturations require knowing the connate water saturation  $S_{wc}$ . In all our examples we use a fourth power of the effective saturation for the relative

water permeability and a quadratic dependence for the steam relative permeability.

The relative permeability functions  $k_{rw}$  and  $k_{rg}$  are considered to be power functions of their respective saturations [7], *i.e.*

$$k_{rw} = \begin{cases} \left( \frac{S_w - S_{wc}}{1 - S_{wc}} \right)^{n_w} & \text{for } S_w \geq S_{wc}, \\ 0 & \text{for } 0 \leq S_w \leq S_{wc}, \end{cases} \quad (82)$$

$$k_{rg} = \left( \frac{S_g}{1 - S_{wc}} \right)^{n_g}.$$

For the computations we take  $n_w = 4$ ,  $n_g = 2$ . The connate water saturation  $S_{wc}$  is given in the table.

The capillary pressure is of the Brooks-Corey type based on the dimensionless capillary pressure from  $P_c(S_w = 0.5) / (\sigma_{wg} \sqrt{\varphi/k}) = 0.5$ . The capillary pressure between steam and water is given by the empirical expression which combines Leverett's approach to non-dimensionalize the capillary pressure [9] with the semi-empirically determined saturation dependence suggested by Brooks [3]:

$$P_c = \sigma_{wg} \gamma \sqrt{\frac{\varphi}{k}} \left( \frac{\frac{1}{2} - S_{wc}}{1 - S_{wc}} \right)^{\frac{1}{\lambda_s}} \left( \frac{S_w - S_{wc}}{1 - S_{wc}} \right)^{-\frac{1}{\lambda_s}}, \quad (83)$$

where  $\gamma$  is a parameter that in many cases assumes values between 0.3 and 0.7. We use  $\gamma = 0.5$  and  $\lambda_s = \frac{1}{2}$ . Finally  $\sigma_{wg} = 0.058$  N/m is the water-vapor interfacial tension. We disregard its temperature dependence and use the value at the boiling point (see [17], p. F-45).

## REFERENCES

- [1] A. Ali Cherif, A. Daïf, *Etude numérique du transfert de chaleur et de masse entre deux plaques planes verticales en présence d'un film de liquide binaire ruisselant sur l'une des plaques chauffée*, Int. J. Heat and Mass Transfer **42** (1999), 2399–2418.
- [2] J. Bear, *Dynamics of Fluids in Porous Media*, p. 650 and 651, Dover Publications, Inc., New York (1972).
- [3] R.B. Bird, W.E. Stewart and E.N. Lightfoot, *Transport Phenomena*, John Wiley & Sons (1960).
- [4] R.H. Brooks and A.T. Corey, *Properties of porous media affecting fluid flow*, J. Irr. Drain. Div., Proc., Am. Soc. Civ. Eng. June (1966), 61-88.

- [5] J. Bruining, D. Marchesin and S. Schechter, *Steam condensation waves in water-saturated porous rocks*, in preparation, 2002.
- [6] J. Bruining, D. Marchesin and C.J. Duijn, *Steam injection into water-saturated porous rock*, IMPA preprint 136/2002, 2002.
- [7] L.P. Dake, *Fundamentals of Reservoir Engineering*, Elsevier Science Publishers, Amsterdam, 1978.
- [8] F.A.L. Dullien, *Porous media; fluid transport and pore structure*, Academic Press, N.Y. (1979).
- [9] E. Isaacson, D. Marchesin, B. Plohr and J.B. Temple, *Multiphase flow models with singular Riemann problems*, Mat. Apl. Comput., **11** 2 (1992), 147-166.
- [10] M. C. Leverett, *Capillary behavior in porous solids*, Trans., AIME, **142** (1941), 142-169.
- [11] O. Oleĭnik, *Discontinuous Solutions of Nonlinear Differential Equations*, Usp. Mat. Nauk. (N.S.) v.12, pp. 3-73, 1957. English transl. in Amer. Math Soc. Transl. Ser. **2** 26, 95-172.
- [12] P.F. Peterson, *Diffusion Layer Modeling for Condensation with Multicomponent Non-condensable Gases*, Journal of Heat Transfer, Transactions of the ASME, Vol **122** (2000), 716-720.
- [13] G.A. Pope, *The application of fractional flow theory to enhanced oil recovery*, SPEJ, 191-205, June 1980.
- [14] M. Prats, *Thermal Recovery*, Monograph Series, SPE, Richardson, TX, **7** (1982).
- [15] S. Schechter, D. Marchesin and B. Plohr, *Classification of codimension-one Riemann solutions*, Journal of Dynamics and Differential Equations, vol. **13** 3 (2001), pp. 523-588.
- [16] A. Shoda, C.Y. Wang and P. Cheng, *Simulation of constant pressure steam injection in a porous medium*, Int. Comm. Heat Mass Transfer Vol **25** 6 (1998), 753-762. (1998).
- [17] W.S. Tortike and S.M. Farouq Ali, *Saturated-steam-property functional correlations for fully implicit reservoir simulation*, SPERE (November 1989) 471-474.
- [18] R.C. Weast, *CRC Handbook of chemistry and physics*, 58<sup>th</sup> edition, CRC Press, Inc. 1977-1978.